Hindawi
International Journal of RF and Microwave Computer-Aided Engineering
Volume 2023, Article ID 4283737, 11 pages
https://doi.org/10.1155/2023/4283737

Research Article

Design of Miniaturized Dual-Mode Antenna for Handset Terminal Communication

Hui Zhang,[1,2,3] **Haofei Shi**,[2] **Yandong Zhang**,[4] **and Zhijuan An**[5]

[1]*Chongqing University, Chongqing 400044, China*
[2]*Chongqing Institute of Green and Intelligent Technology, Chinese Academy of Sciences, Chongqing 400714, China*
[3]*Chongqing School, University of Chinese Academy of Sciences, Chongqing 400714, China*
[4]*School of Electronic Engineering, Xi'an University of Posts and Telecommunications, Xi'an 710121, China*
[5]*School of Physics, Xidian University, Xi'an 710071, China*

Correspondence should be addressed to Hui Zhang; zhanghui@xastarnet.com

Received 19 January 2023; Revised 5 May 2023; Accepted 31 May 2023; Published 8 June 2023

Academic Editor: A. K. Gautam

Copyright © 2023 Hui Zhang et al. This is an open access article distributed under the Creative Commons Attribution License, which permits unrestricted use, distribution, and reproduction in any medium, provided the original work is properly cited.

This paper presents a miniaturized dual-mode handset antenna design. A quadrifilar helix antenna (QHA) is utilized to work at higher band (1980-2010 MHz and 2170-2200 MHz) with circular polarization. By cutting off a circular slot on the outer conductor of the QHA feedline and introducing four quarter-wavelength short-circuited stubs, the QHA radiator and its feedline can also work as a monopole antenna at lower band (440-560 MHz) with linear polarization. With this radiator-sharing technique, the dual-mode characteristics can be achieved utilizing only a QHA; therefore, the antenna dimension can be reduced remarkably since it is unnecessary to design an additional monopole antenna. Moreover, the short-circuited stubs are designed with stripline and integrated with the one-to-four power divider and phase shifter for further miniaturization. The measured S11 is less than -8 dB. The typical gain is higher than 0.5 dBi at lower band and 2.5 dBi at higher band. The AR of the QHA is better than 1.3 dB, and the head SAR values are much lower than the international standard at both lower and higher bands. The proposed miniaturized dual-mode antenna can be applied to portable handsets to realize the intercom and satellite communications.

1. Introduction

Satellite communication can achieve stable and seamless global coverage, but its operation costs and power consumption are very high [1]. Intercom communication, by contrast, is low-cost and easy to realize self-organizing network but has a short communication distance. Therefore, integration of intercom and satellite communication modules on a handset terminal is of important practical significance, which correspondingly places a greater demand on the handset antenna. In intercom communication, the antenna works at lower band of UHF and is required to radiate omnidirectionally on the horizontal plane with linear polarization; hence, the monopole antenna is often utilized since its length is only one half of the dipole antenna. In satellite communication, the antenna works at higher band of UHF, and the QHA is often adopted due to its better circular polarization characteristics and wider beamwidth in upper half-space. Presently, most researches are concentrated on the individual design of monopole antennas or QHAs. In [2], a meander-line-folded monopole antenna at 450 MHz was proposed with a sliding via for tuning over the lower UHF band (412-475 MHz). The antenna has low profile due to the adoption of meander-line structure; however, its maximum measured gain is only -6.1 dBi. A conformal broadband monopole antenna composed of an open ring ground and a circular monopole patch was presented in [3], which can work at the frequency band of 98 MHz to 622 MHz. However, the antenna has a dimension of $0.25\lambda \times 0.25\lambda$ at the minimum frequency and therefore is too large for handset application. In [4], a slim monopole antenna with two parasitic strips on both sides is presented. By adding novel in-body structures to the three strips, it can achieve wider impedance and radiation pattern bandwidths.

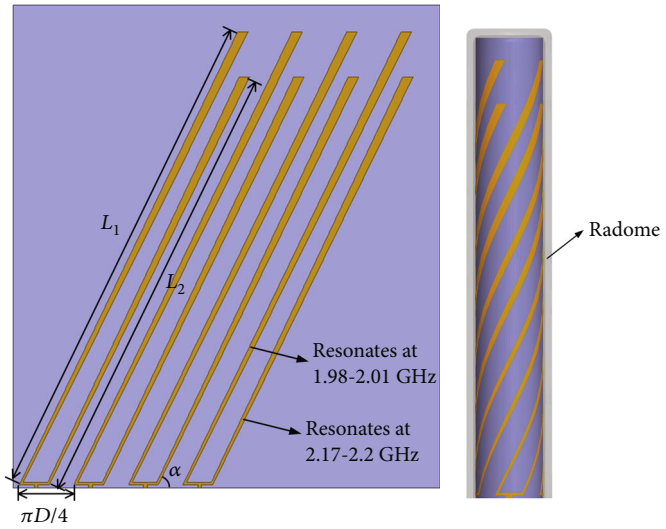

FIGURE 1: Configuration of improved QHA. (a) Unwrapped model. (b) 3D model.

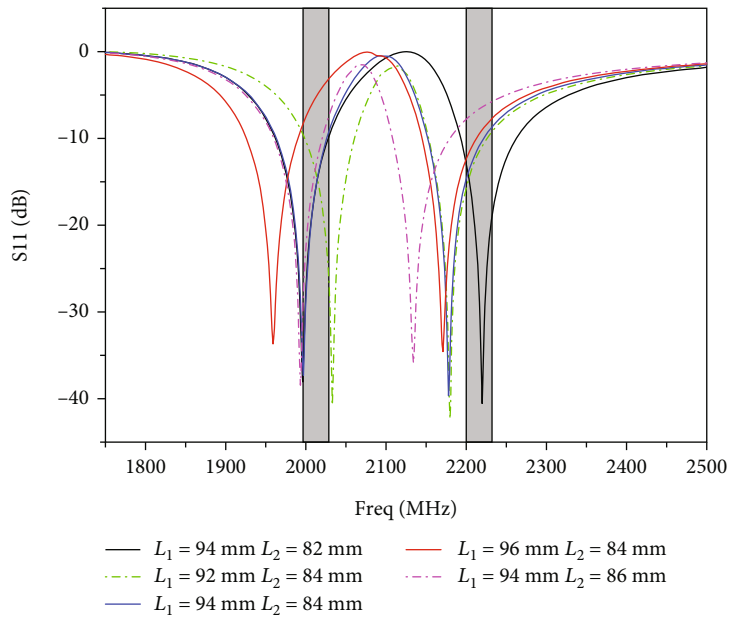

FIGURE 2: Simulated S11 for different arm lengths of L_1 and L_2 at higher band.

In [5], a slot helix antenna working at GPS L1 and L2 bands was proposed, which consists of six helix radiation arms with double-faced slot radiation structure and can therefore realize dual-band radiation with good performance. A dual-band spiral printed QHA was presented in [6], which is miniaturized by inserting dielectric loading inside the helix, covering the radiation elements with dielectric sealants and turning the radiation elements into the form of parallelogram spirals. In [7], a pattern reconfigurable circularly polarized QHA was presented. By controlling the phase between two composed bifilar helices, it can generate cardioid patterns toward both ends, vertical toroid patterns in different orientations and mixed patterns of cardioid and toroid at several global navigation satellite system (GNSS) bands.

TABLE 1: Structure parameters of improved QHA.

Parameter	D (mm)	α (°)	L_1 (mm)	L_2 (mm)
Value	13	64	94.3	84

However, for handsets integrated with intercom and satellite communication modules, the total antenna size may be too large to be portable if the two antennas are designed independently. On the other hand, the independent design may also cause strong mutual coupling if the two antennas

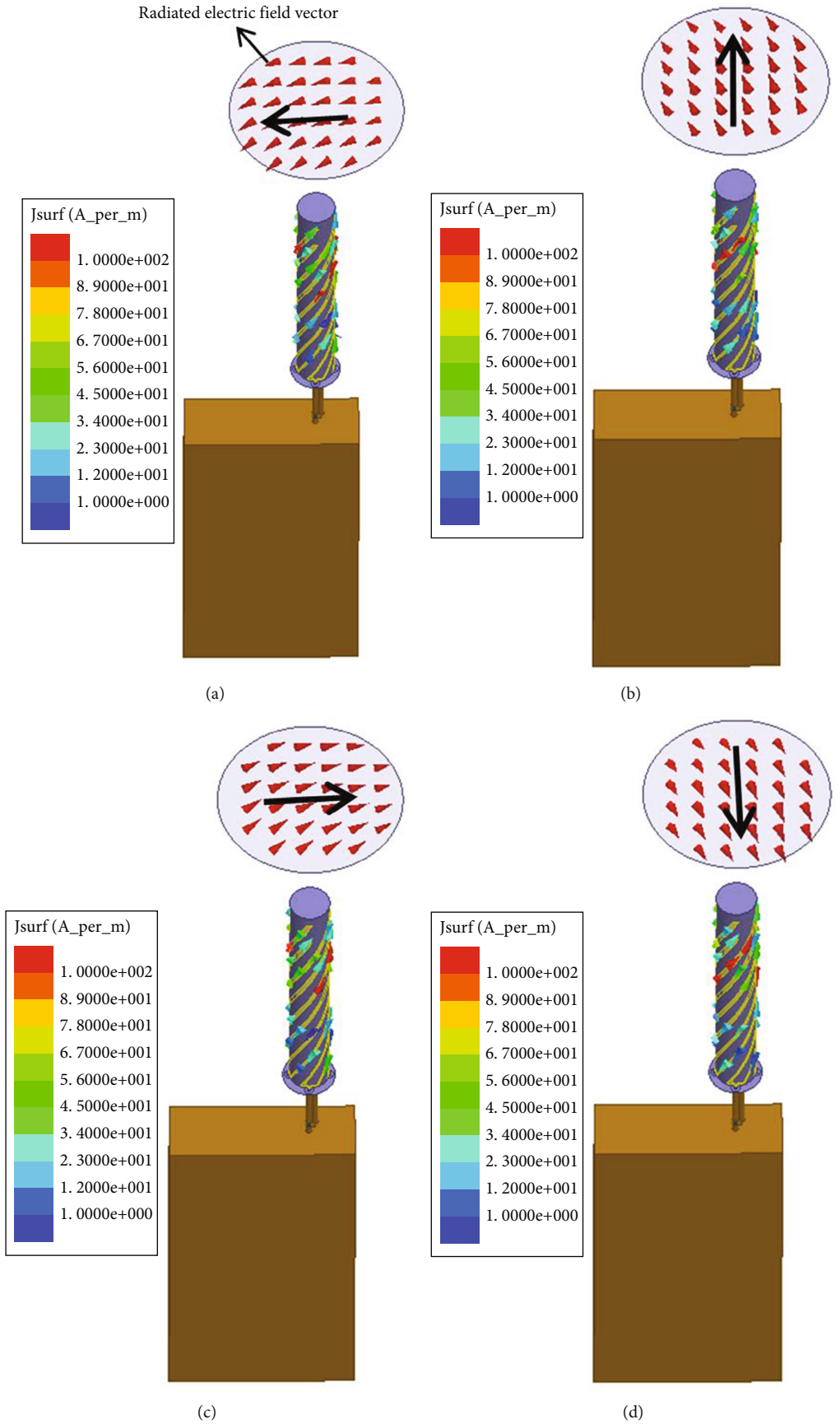

FIGURE 3: Simulated surface current and radiated electric field distributions of QHA at 1.995 GHz: (a) 0°, (b) 90°, (c) 180°, and (d) 270°.

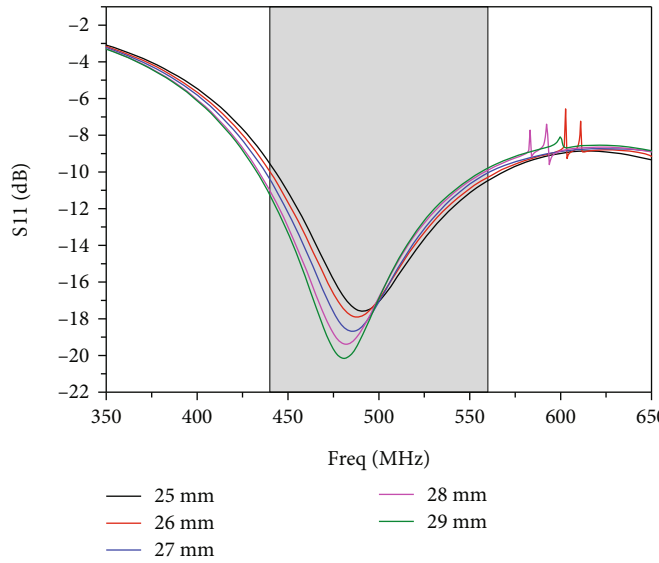

Figure 4: Simulated S11 for different lengths of QHA feedline at lower band.

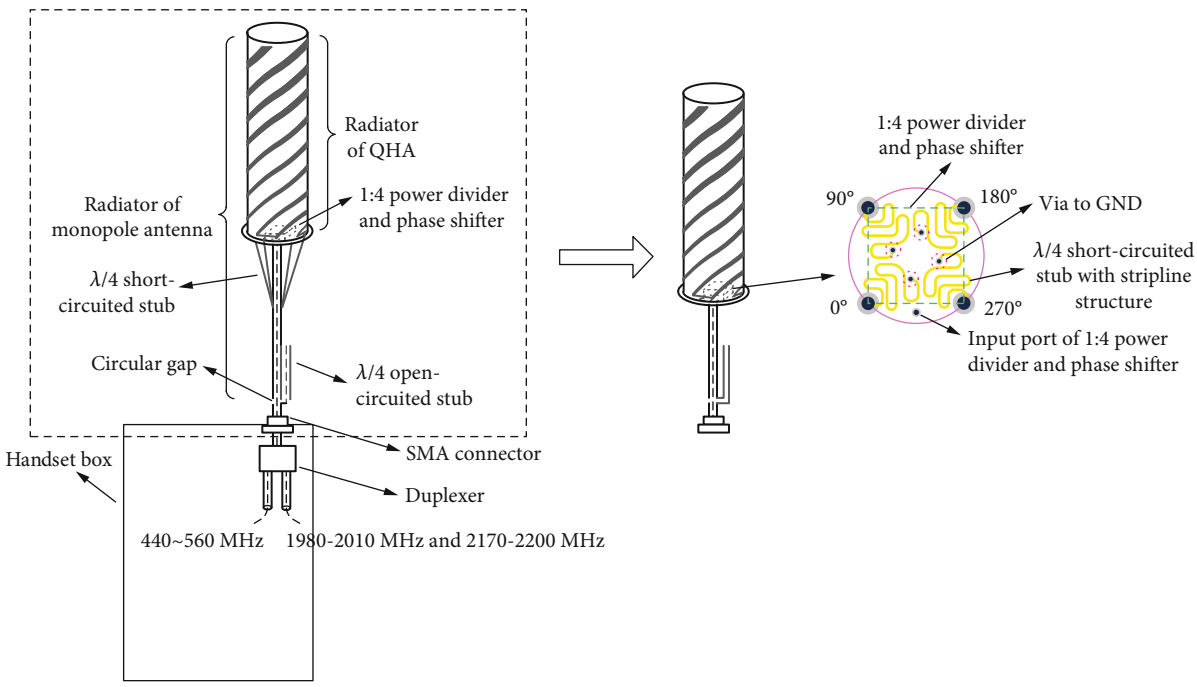

Figure 5: Geometry of miniaturized dual-mode handset antenna.

are not arranged reasonably [8–10]. To solve these problems, the integrated and miniaturized design of the QHA and the monopole antenna is required. In [11], the monopole antenna, dipole antenna, and QHA are integrated coaxially to achieve multimode and multifrequency. However, the miniaturization is not taken into account, and the two-port design of the antenna also results in a high complexity. In [12], a wide band monopole antenna working at UHF clustered with two wide band dipole antennas working at L and S bands is proposed. [13] presents a design approach of a multiband and wideband antenna consisting of a monopole, a folded loop, and a helix. [14] presents a compact, dual-polarized, multiband four-port flexible MIMO antenna. In [15], a miniaturized dual-band and dual-polarized base station antenna loaded with a duplex balun is proposed. The antenna has two independent current paths, which enables it to operate in dual bands. In addition, the two paths are bent for miniaturization. [16] presents a compact dual-band circularly polarized microstrip patch antenna. By the utilization of dual-frequency coplanar patch and metal capacity-loaded technology, the antenna dimension can be reduced. A dual-band dual-circularly polarized shared-aperture antenna for

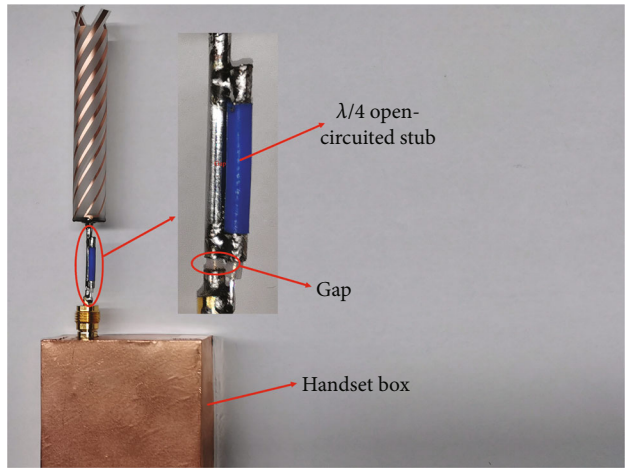

Figure 6: Photograph of the fabricated antenna.

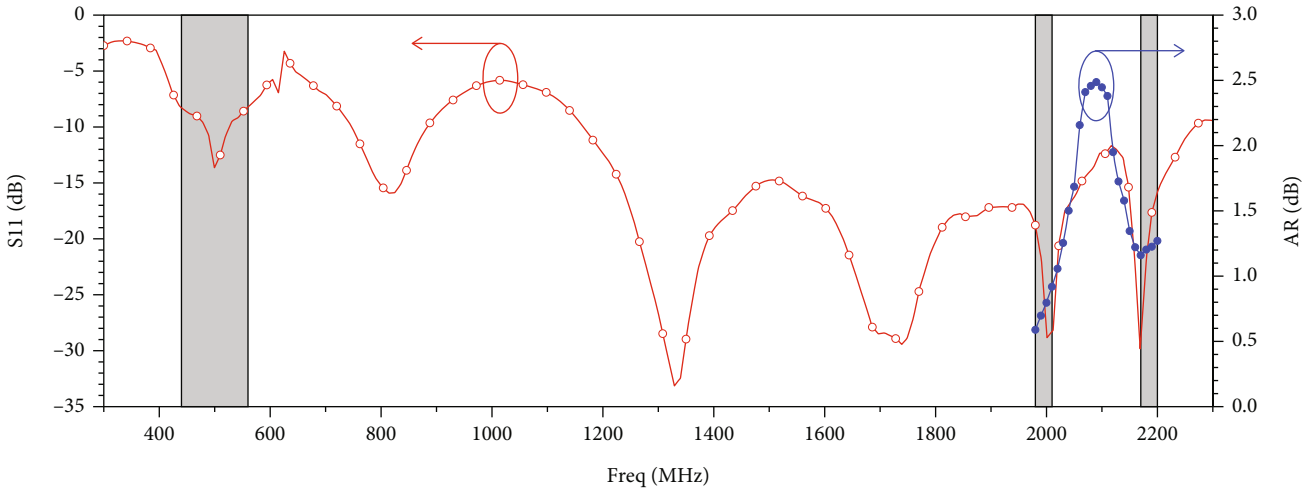

Figure 7: Measured S11 and AR with frequency.

UHF and millimeter-wave bands is proposed in [17]. The metal ground of millimeter-wave reflectarray is reused as the UHF radiation patch to realize the dual-band shared-aperture. However, these antennas mentioned above can only operate with either linear or circular polarization mode. In [18], a dual-band handset antenna is designed. The antenna consists of a QHA working at S band (1.9-2.2 GHz) with circular polarization and a monopole antenna at UHF band (420-520 MHz) with linear polarization, which are arranged coaxially to realize miniaturization. But the diameter of the antenna is still too large, and the gain at S band is relatively low.

A miniaturized design of the dual-mode handset antenna is presented in this paper. By utilizing the radiator-sharing technique, the QHA can work at both higher band (1980-2010 MHz and 2170-2200 MHz) with circular polarization and lower band (440-560 MHz) with linear polarization simultaneously. In the case of plastic handset box, another design scheme of dual-port feeding is proposed, which has the advantage of lower insertion loss.

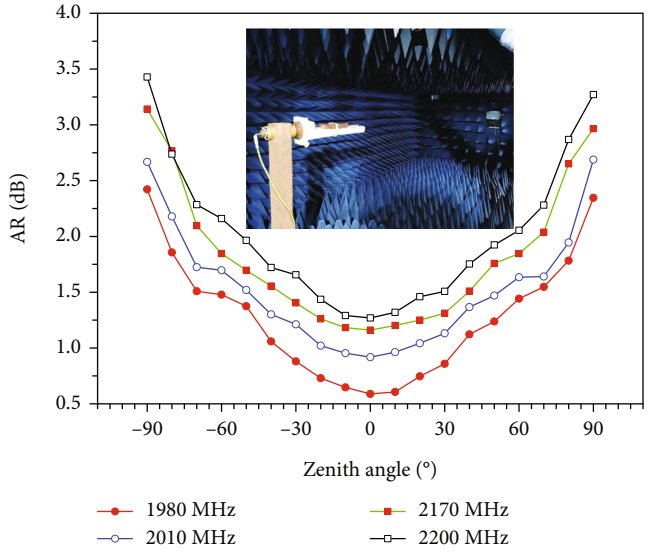

Figure 8: Measured AR with zenith angle.

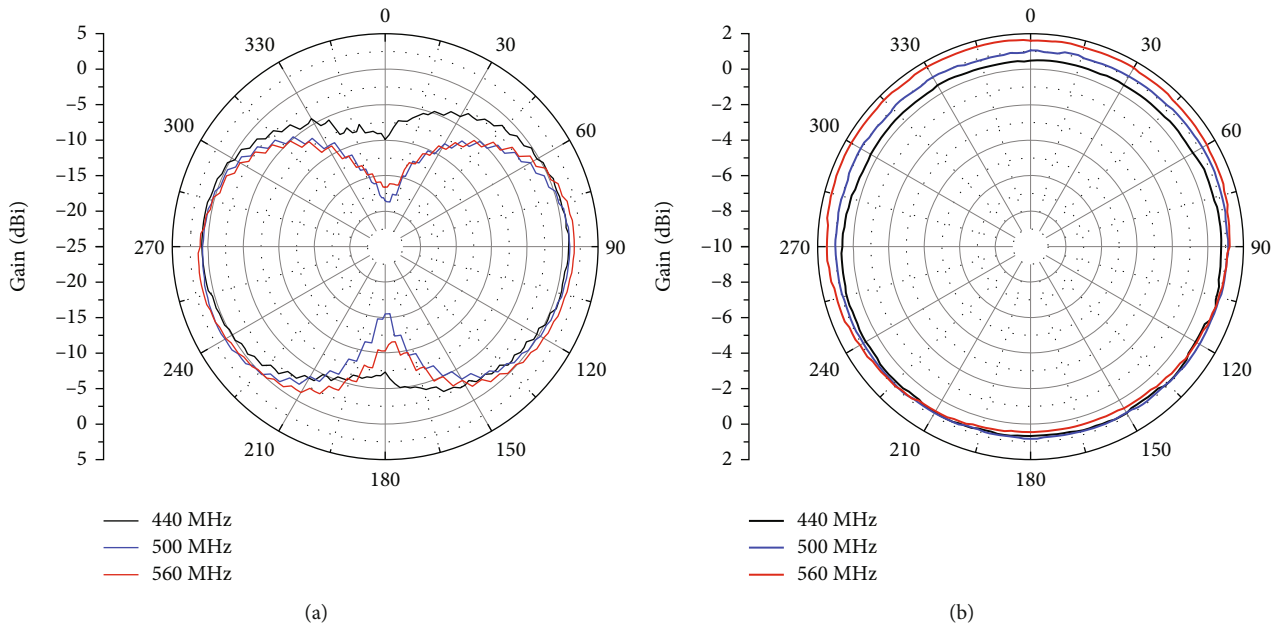

FIGURE 9: Measured radiation pattern at lower band. (a) *E*-plane. (b) *H*-plane.

2. Miniaturized Design of Dual-Mode Handset Antenna

At higher band, the QHA is utilized to realize circular polarization and wider beamwidth in upper half-space. It has a diameter of D and is covered with a cylindrical radome made of PC/ABS; the thickness of the radome is 1 mm. For the sake of uplink and downlink transmission, each radiating arm of the QHA is developed into two arms with different lengths to achieve double resonance [19]. The longer arm with a length of L_1 resonates at 1980-2010 MHz and the shorter one with a length of L_2 at 2170-2200 MHz, as shown in Figure 1, where Figures 1(a) and 1(b) represent the unwrapped and 3D model, respectively. The resonating curves for different arm lengths of L_1 and L_2 are displayed in Figure 2. It is shown that when $L_1 = 94$ mm and $L_2 = 84$ mm, the QHA can resonate at the desired band of 1980-2010 MHz and 2170-2200 MHz. In addition, the width of each arm is designed to be linearly tapered from 0.7 mm to 1.5 mm to increase the impedance bandwidth. The final structure parameters of the improved QHA is listed in Table 1.

To achieve the circular polarization, a one-to-four power divider and phase shifter is connected to the four input ports of the QHA to realize the feeding with equal amplitude and 90° phase difference. In accordance with the analysis in [20], the QHA can be equivalent to two orthogonal small loop-dipole antennas fed in quadrature phase. As a result, the radiated electric field components E_θ and E_ϕ are of equal amplitude and have a 90° phase difference; therefore, a circular polarization pattern can be excited. To illustrate this, the surface current distributions on the four arms for different phases of 0°, 90°, 180°, and 270° at 1.995 GHz are simulated and displayed in Figures 3(a)–3(d), and the corresponding radiated electric field vectors along the axis direction are also shown in these figures. It is clear that the radiated electric field vectors change with time and rotate in a clockwise manner, which means that a left-hand circular polarization wave is excited.

To realize linear polarization and omnidirectional radiation at lower band, the monopole antenna is utilized generally since its length is only one half of the dipole antenna. However, if the monopole antenna is designed separately, the total antenna size will be larger. To solve this problem, at the start section of the QHA feedline, its outer conductor is cut off with a circular gap engraved, and an open-circuited stub with a length of quarter-wavelength of higher band is connected to the disconnection. For higher band, the disconnection presents a short-circuited state due to the introduction of the quarter-wavelength open-circuited stub, which keeps the continuity of feeding current and has little effect on the feeding of the QHA, whereas for lower band, the disconnection makes the feeding current flowing along the outer conductor of the QHA; therefore, the outer conductor of the QHA feedline can act as a monopole antenna and work with linear polarization pattern at lower band. With this design scheme, we can utilize one QHA to realize dual-frequency and dual-mode simultaneously.

Since the QHA feedline acts as a monopole antenna, its length should be long enough to resonate at lower band. For the sake of miniaturization, four input ports of the QHA are connected to the outer conductor of its feedline by four stubs with a length of quarter-wavelength of higher band. For higher band, it is equivalent to connect four input ports of the QHA in parallel with a quarter-wavelength short-circuited stub, which therefore has little effect on its current distribution due to the impedance transformation, whereas for lower band, the feeding current can flow from the outer conductor of the QHA feedline to four radiating arms of the QHA via the four stubs. That is, four radiating arms of the QHA not only act as the QHA radiator but

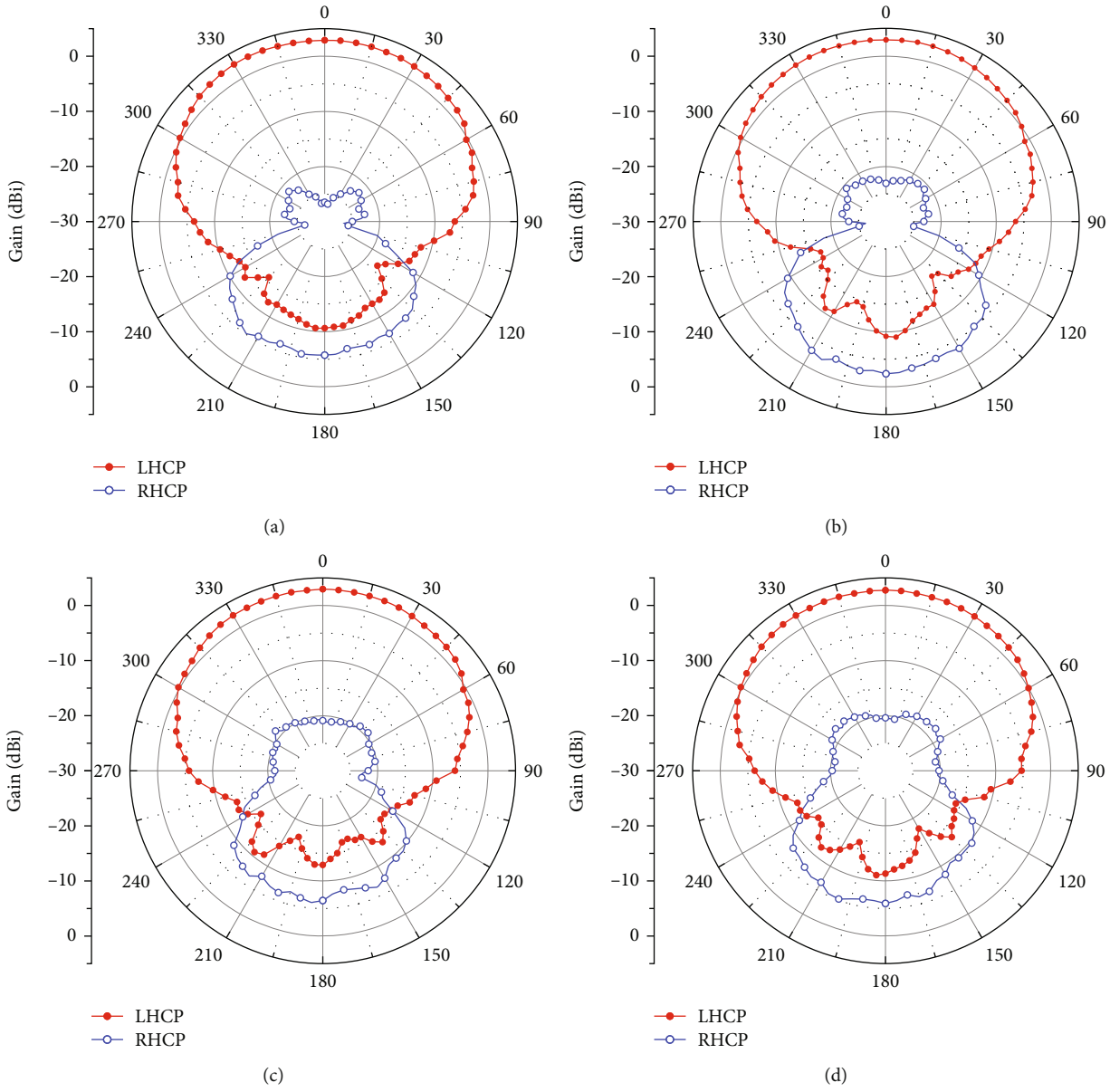

Figure 10: Measured radiation pattern at (a) 1980 MHz, (b) 2010 MHz, (c) 2170 MHz, and (d) 2200 MHz.

constitute the monopole antenna radiator together with the QHA feedline; therefore, the length of the QHA feedline as well as the total antenna size can be reduced remarkably with this radiator-sharing technique. Since the length of the QHA's radiating arms is determined by the resonating frequency at higher band and cannot be changed, therefore by adjusting the length of the QHA feedline, the proposed antenna can resonate at the desiring lower band. Figure 4 displays the simulated S11 for different lengths of the QHA feedlines, which shows that when the QHA feedline is 27 mm long, the simulated S11 is below -10 dB over the frequency range of 440-560 MHz. It is noted that there are some burrs on the curve near the frequency of 600 MHz, which is caused by the coupling of two radiating arms with different lengths.

To miniaturize the antenna further, the four quarter-wavelength short-circuited stubs are designed with stripline structure and integrated with the one-to-four power divider and phase shifter using multilayer PCB. Finally by connecting the QHA feedline to the intercom and satellite communication modules on the terminal mainboard, respectively, via a duplexer, a miniaturized dual-mode handset antenna can be obtained, the configuration of which is shown in Figure 5.

3. Results and Discussion

In accordance with the design scheme described above, a miniaturized dual-mode antenna for handset terminal communication is fabricated with a size of 128 mm $(H) \times 13$ mm (D), as shown in Figure 6. The measured S11 and AR with frequency are displayed in Figure 7. It is shown that the S11 is less than -8 dB at 440-560 MHz band and -15 dB at 1980-2010 MHz and 2170-2200 MHz bands, while the

Table 2: Antenna efficiency at different frequencies.

Frequency (MHz)	440	500	560	1980	1995	2010	2170	2185	2200
Antenna efficiency	73.4%	79.2%	84.6%	62.5%	62.7%	63.4%	66.8%	67.2%	69.3%

Table 3: Comparison of the proposed antenna with the previous works.

Ref.	Dimension (mm^2)	Number of ports	Bandwidth (MHz)	VSWR or S11	Gain (dBi)	Pattern	Polarization	AR (dB)
[12]	155 (L) × 69.5 (W)	Multiport	380~780	VSWR < 3	2.94	Omnidirectional radiation	Linear	/
			1230~1620	VSWR < 2	6.29	Endfire radiation	Linear	/
			1700~2340	VSWR < 2	6.76	Endfire radiation	Linear	/
[13]	41 (L) × 18 (W)	Single-port	800~960	VSWR < 3	2.5	Omnidirectional radiation	Linear	/
			1700~2500	VSWR < 3	4.1	Approximate omnidirectional radiation	Linear	/
[18]	254 (H) × 38.1 (D)	Dual-port	225~512	Not given	2.0	Omnidirectional radiation	Linear	/
			1164~1300 1559~1626	S11 < −9 dB	0.8	Upper half-space radiation	Circular	Not given
This work	128 (H) × 13 (D)	Single-port	440~560	S11 < −8 dB	1.69	Omnidirectional radiation	Linear	/
			1980~2010 2170~2200	S11 < −15 dB	3.03	Upper half-space radiation	Circular	<1.3

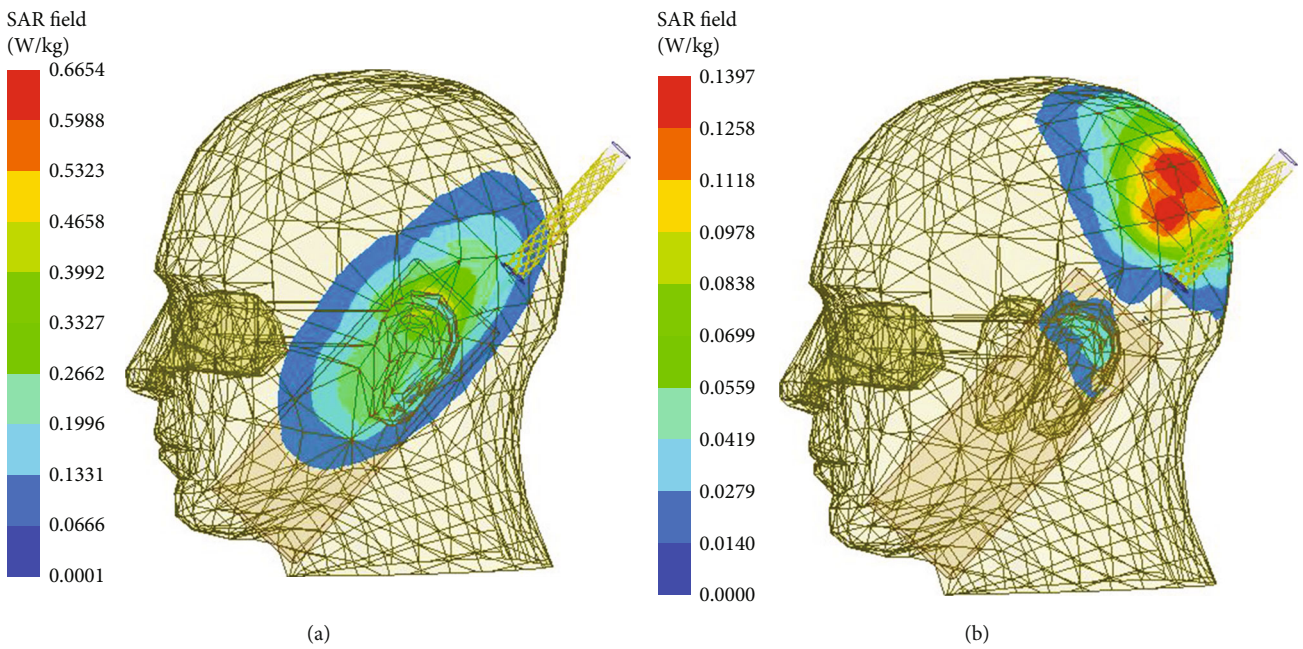

Figure 11: Simulated SAR at (a) 500 MHz and (b) 1995 MHz.

AR is better than 1.3 dB, which means a good matching and circular polarization performance over the whole working band. It is noted that the S11 is less than -10 dB over the nonworking frequency range of 1170-1980 MHz, which is due to the loss caused by the isolating resistor in the one-to-four power divider and phase shifter. The measured AR for different zenith angles is measured and shown in Figure 8. It is observed that the 3 dB AR beamwidth can approximately cover the whole upper half-space. Figures 9(a) and 9(b) display the measured E-plane and H-plane radiation patterns at lower band, respectively. The E-plane patterns have "∞" shape, and the H-plane patterns are approximately omnidirectional with the gain greater than 0.5 dBi. Due to the asymmetry of the handset box, an out-of-roundness of about 1 dB can be seen from the H-plane pattern. Figures 10(a)–10(d) display the measured

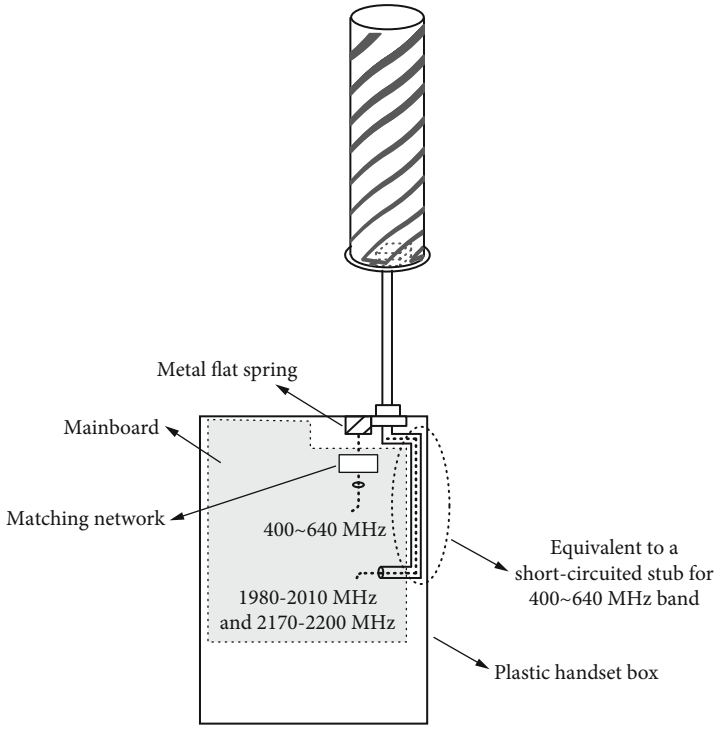

Figure 12: Geometry of handset antenna with plastic box.

radiation pattern at higher band of 1980 MHz, 2010 MHz, 2170 MHz, and 2200 MHz, respectively. It can be shown that the antenna exhibits a wider beamwidth on the upper half-space and the peak gain is higher than 2.5 dBi. In addition, the cross polarization isolation is greater than 20 dB, which also means a better circular polarization performance. The antenna efficiency at different frequencies is listed in Table 2. At lower band of 440-560 MHz, it is greater than 73%, and at higher band of 1980-2010 MHz and 2170-2200 MHz, it varies over the range of 62.5%-69.3%.

Furthermore, a comparison between the proposed antenna and the reference antennas is listed in Table 3. The antennas in [12, 13] radiate linear polarization waves with endfire or approximate omnidirectional pattern, instead of circular polarization waves with upper half-space radiation pattern as needed in the satellite communication. The antenna in [18] works with circular polarization and upper half-space radiation pattern; however, the diameter of it is too large and the antenna gain at higher band is relatively low. Compared with the reference antennas, the proposed antenna not only works with dual-band and dual-polarization mode but has a higher gain with a smaller diameter.

To evaluate the effect of the handset on the user's head, the 1 g spatial-average head SAR of the proposed antenna at 500 MHz and 1995 MHz is simulated, as shown in Figures 11(a) and 11(b). In the simulation, the gap between the ear and the handset is 2 mm, which is quite close to practical scenarios. The input transmit power for SAR calculation is 24 dBm at both frequencies. It can be found that the simulated SAR values are much lower than the industry specified SAR limit of 1.6 W/kg for 1 g tissue [21] at both lower and higher frequencies.

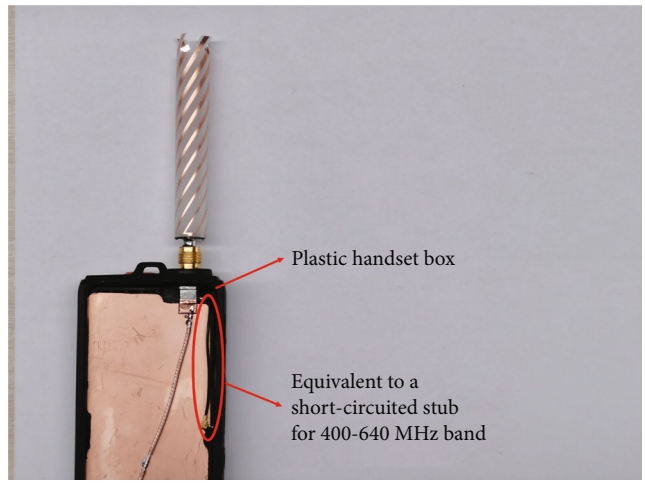

Figure 13: Photograph of the fabricated antenna.

In practice, it often occurs that the handset box is made of plastic material. In this case, the dual-port feeding technique can be utilized. The QHA is still coaxial fed with its radiator remains unchanged, whereas for the monopole antenna, its feeding point is shifted to the terminal mainboard and connected with the base of the SMA connector via a metal flat spring, as shown in Figure 12. Since it is unnecessary to use the duplexer, therefore, the insertion loss can be reduced compared with the single-port feeding technique described above. To realize the impedance matching

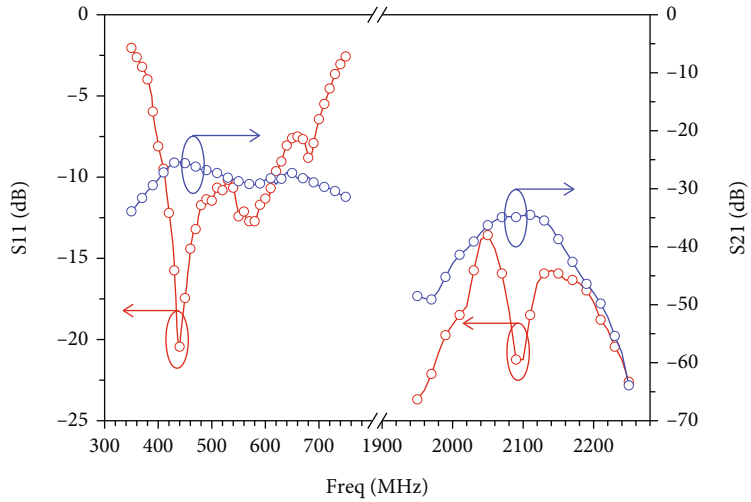

Figure 14: Measured S11 and port isolation.

Table 4: Antenna efficiency and gain at different frequencies.

Frequency (MHz)	400	520	640	1980	1995	2010	2170	2185	2200
Antenna efficiency	68.6%	77.4%	81.7%	63.8%	64.1%	64.7%	68.2%	68.6%	70.5%
Antenna gain (dBi)	0.77	1.09	1.53	3.15	3.21	3.23	3.14	3.06	2.95

of the monopole antenna, it is required to add an LC matching network on the mainboard. Note that the outer conductor of the QHA feedline below the connector is equivalent to a short-circuited stub for the monopole antenna, and therefore, it behaves as a part of the matching network. The antenna is fabricated as shown in Figure 13. Its VSWR and the port isolation are measured with the results displayed in Figure 14. It is clear that the measured bandwidth of the monopole antenna with S11 less than -8 dB is 400-640 MHz. The isolation between the two ports exceeds 25 dB, which means a small mutual coupling between the monopole antenna and the QHA. The antenna efficiency and gain at different frequencies are listed in Table 4. Compared with the single-port antenna described in Section 2, at lower band, the antenna efficiency is slightly lower due to the matching network, whereas at higher band, it is slightly higher since there is no disconnection on the feedline.

4. Conclusions

This paper proposes a miniaturized design of dual-mode handset antenna. The antenna works at 440-560 MHz with linear polarization and at 1980-2010 MHz and 2170-2200 MHz with circular polarization. The measured results show that the proposed antenna has the advantages of single port, small size, wide bandwidth, and high gain. In addition, for handsets with plastic box, we present another design scheme, which has lower insertion loss without the use of the duplexer. The proposed antennas are good candidates for portable handset terminal communication.

Data Availability

The data used to support the findings of this study are available from the corresponding author upon reasonable request.

Conflicts of Interest

The authors declare that they have no conflicts of interest.

References

[1] F. Davarian, S. Asmar, M. Angert et al., "Improving small satellite communications and tracking in deep space—a review of the existing systems and technologies with recommendations for improvement. Part II: small satellite navigation, proximity links, and communications link science," *IEEE Aerospace and Electronic Systems Magazine*, vol. 35, no. 7, pp. 26–40, 2020.

[2] A. Loutridis, M. John, and M. J. Ammann, "Folded meandered monopole for emerging smart metering and M2M applications in the lower UHF band [wireless corner]," *IEEE Antennas and Propagation Magazine*, vol. 58, no. 2, pp. 60–65, 2016.

[3] P. Liu, C. Wang, and Q. Zhu, "A conformal broadband monopole antenna for VHF/UHF band applications," in *13th International Symposium on Antennas, Propagation and EM Theory*, Zhuhai, China, 2021.

[4] D. J. Qin, B. H. Sun, and R. Zhang, "VHF/UHF ultrawideband slim monopole antenna with parasitic loadings," *IEEE Antennas and Wireless Propagation Letters*, vol. 21, no. 10, pp. 2050–2054, 2022.

[5] Y. H. Yang, J. L. Guo, B. H. Sun, and Y. H. Huang, "Dual-band slot helix antenna for global positioning satellite applications,"

IEEE Transactions on Antennas and Propagation, vol. 64, no. 12, pp. 5146–5152, 2016.

[6] Y. N. Han, H. L. Wang, Z. W. Wang et al., "Dual-band spiral printed quadrifilar helical antenna miniaturized by surface and inner dielectric loading," *IEEE Access*, vol. 7, pp. 30244–30251, 2019.

[7] W. Sun, G. D. Su, L. L. Sun, and X. Chen, "A pattern reconfigurable circularly polarized quadrifilar helix antenna through phase control," *IEEE Transactions on Antennas and Propagation*, vol. 70, no. 9, pp. 7766–7773, 2022.

[8] L. Duggani, U. Naik, and V. Rayar, "Review of mutual coupling reduction in microstrip patch antenna array for MIMO applications," in *2020 3rd International Conference on Intelligent Sustainable Systems (ICISS)*, Thoothukudi, India, 2020.

[9] S. Kim and S. Nam, "A compact and wideband linear array antenna with low mutual coupling," *IEEE Transactions on Antennas and Propagation*, vol. 67, no. 8, pp. 5695–5699, 2019.

[10] Á. Palomares-Caballero, A. Alex-Amor, J. F. Valenzuela-Valdés, and P. Padilla, "Helix antenna array based on higher symmetries for antenna miniaturization and mutual coupling reduction," in *2019 IEEE-APS Topical Conference on Antennas and Propagation in Wireless Communications (APWC)*, Granada, Spain, 2019.

[11] W. Zhao, L. Xu, and C. C. Dong, "A multi-mode and multi-frequency handset antenna," in *2016 11th International Symposium on Antennas, Propagation and EM Theory (ISAPE)*, Guilin, China, 2016.

[12] J. Zhang, S. Zhang, and G. F. Pedersen, "A wide band compact size UHF band monopole clustered with L and S band dipoles for self-networking communication in handset devices," in *12th European Conference on Antennas and Propagation (EuCAP 2018)*, London, UK, Apr. 2018.

[13] Y. J. Ren, J. Ren, and H. S. Hwang, "General design approach of monopole and helix integrated antennas for radio apparatus," *Microwave and Optical Technology Letters*, vol. 57, no. 7, pp. 1718–1723, 2015.

[14] J. Kulkarni, A. G. Alharbi, I. Elfergani, J. Anguera, C. Zebiri, and J. Rodriguez, "Dual polarized, multiband four-port decagon shaped flexible MIMO antenna for next generation wireless applications," *IEEE Access*, vol. 10, pp. 128132–128150, 2022.

[15] J. Li, J. Li, J. Yin, C. Guo, H. Zhai, and Z. Zhao, "A miniaturized dual-band dual-polarized base station antenna loaded with duplex baluns," *IEEE Antennas and Wireless Propagation Letters*, pp. 1–5, 2023.

[16] X. Li, R. Ma, H. Cai, Y. M. Pan, and X. Y. Zhang, "High-gain dual-band aperture-shared CP patch antenna with wide AR beamwidth for satellite navigation system," *IEEE Antennas and Wireless Propagation Letters*, pp. 1–4, 2023.

[17] H. Zheng, S. Li, C. Wang, and W. Cao, "Dual-band dual-circularly polarized shared-aperture antenna for UHF-wave and millimeter-wave applications," in *2022 Cross Strait Radio Science & Wireless Technology Conference (CSRSWTC)*, Haidian, China, 2022.

[18] P. G. Elliot, E. N. Rosario, and R. J. Davis, "Novel quadrifilar helix antenna combining GNSS, iridium, and a UHF communications monopole," in *MILCOM 2012 - 2012 IEEE Military Communications Conference*, Orlando, FL, USA, 2012.

[19] Y. D. Yan, Y. C. Jiao, R. Tian, and W. Zhang, "A dual-band circularly-polarized quadrifilar helix antenna," in *11th UK-Europe-China Workshop on Millimeter Waves and Terahertz Technologies*, HangZhou, China, 2018.

[20] C. C. Kilgus, "Multielement, fractional turn helices," *IEEE Transactions on Antennas and Propagation*, vol. 16, no. 4, pp. 499-500, 1968.

[21] IEEE International Committee on Electromagnetic Safety, "IEEE standards for safety levels with respect to human exposure to electric, magnetic, and electromagnetic fields, 0 Hz to 300 GHz," IEEE Std C95.1-2019, 2020.